A&A, 712, L8 (2026)
https://doi.org/10.1051/0004-6361/202661107

Astronomy & Astrophysics

Letter to the Editor

Feeding and feedback in dwarf galaxies (FeeD)

I. Evidence of nuclear ultra-fast and galaxy-scale outflows in the dwarf galaxy Arp 151

S. Mondal[1,2,★], A. Patel[2], M. Mezcua[3,4], R. Joshi[2], Y. Xu[3,4], K. Aditya[5], S. Subramanian[2], and V. Rodriguez Morales[3]

[1] Department of Physics and Electronics, Christ University, Bangalore 560029, India
[2] Indian Institute of Astrophysics, II Block, Koramangala, Bangalore 560034, India
[3] Institute of Space Sciences (ICE, CSIC), Campus UAB, Carrer de Can Magrans, s/n, 08193 Barcelona, Spain
[4] Institut d'Estudis Espacials de Catalunya (IEEC), Edifici RDIT, Campus UPC, 08860 Castelldefels, Barcelona, Spain
[5] Raman Research Institute, C. V. Raman Avenue, 5th Cross Road, Sadashivanagar, Bengaluru 560080, India

Received 25 May 2026 / Accepted 22 June 2026

ABSTRACT

Feeding and feedback regulated by supermassive black holes play a central role in galaxy growth and evolution, yet these processes remain poorly understood in low-mass galaxies. In particular, the presence, properties, and role of nuclear ultra-fast outflows (UFOs) in low-mass galaxy systems are largely unexplored. We analyzed available *NuSTAR* X-ray observations of Arp 151 and find possible evidence ($\sim 2\sigma$ confidence) of a fast outflow with a velocity of $\sim 0.18c$ from the central black hole. Furthermore, we have detected an optical galaxy-scale outflow in MaNGA integral field unit data. The estimated nuclear and galaxy-scale mass outflow rates are $\sim 0.015\,M_\odot$/yr from *NuSTAR* and $\sim 0.43\,M_\odot$/yr from MaNGA, respectively. Our estimates suggest that such outflows may significantly regulate the feedback process in the galaxy. A comparison of the kinetics of the UFO and the galaxy-scale outflow indicates that they are in the momentum-conserving phase. This tentative discovery implies that dwarf galaxies are also able to generate UFOs, which so far have been detected in massive galaxies. Thus, the active galactic nucleus feedback may also be important for the evolution of the dwarf galaxies.

Key words. ISM: jets and outflows – galaxies: active – galaxies: dwarf – galaxies: individual: Arp 151

1. Introduction

Active galactic nuclei (AGNs) are powered by the accretion of matter onto supermassive black holes (SMBHs; $\sim 10^{6-10}\,M_\odot$) at the centers of massive galaxies. During this process, a large amount of energy is released in the form of radiation, relativistic jets, and outflows (OFs), which can interact with the interstellar medium of the host galaxy. This is commonly known as AGN feedback, which can heat or expel gas from the galaxy, thereby regulating star formation and influencing the growth of both the SMBH and its host galaxy (Silk & Rees 1998; Fabian 2012).

The effect of feeding and feedback mechanisms is poorly understood for massive black holes (BHs; 10^5–$10^6\,M_\odot$) in dwarf galaxies (with stellar masses $<10^{9.5}\,M_\odot$). Compared to massive galaxies, AGNs in dwarf systems tend to be fainter and less powerful (see Mezcua et al. 2024). The AGN feedback may play a crucial role in regulating star formation in dwarf galaxies and is an important testbed of galaxy formation and cosmology (Koudmani et al. 2021 and references therein). Furthermore, if the BHs in these systems grow efficiently, they can have more of an effect on the host galaxy (Barai & de Gouveia Dal Pino 2019; Koudmani et al. 2021). Recent studies have found direct evidence of spatially extended high-velocity ionized gas OFs in dwarf galaxies consistent with AGN-driven OFs (Manzano-King et al. 2019; Rodríguez Morales et al. 2025; Salehirad et al. 2025).

There is a growing body of evidence for the presence of (sub)relativistic ($\gtrsim 0.1c$) OFs in the X-ray spectra of AGNs in massive galaxies, imprinted by blueshifted Fe K-shell absorption lines from Fe XXV and/or Fe XXVI at rest-frame energies >7 keV (Papadakis et al. 2007; Sim et al. 2010; Tombesi et al. 2010; Matzeu et al. 2023 and references therein). These lines have been observed in a highly ionized medium with a column density $\geq 10^{22}\,\mathrm{cm}^{-2}$ and a blueshifted velocity $\gtrsim 0.2c$ (Pounds et al. 2003; Cappi 2006; Braito et al. 2007); they are known as ultra-fast outflows (UFOs). The kinetic power of UFOs can significantly influence the host galaxy environment and thus their evolution (Tombesi et al. 2013 and references therein), consistent with the SMBH-galaxy feedback driven by OFs (King & Pounds 2003; Gaspari et al. 2011).

However, no such evidence of UFOs from the inner central engine has been reported in dwarf galaxies, which can be the regulator of the feeding and feedback process. These massive BHs might be the counterparts of the seed BHs formed in the early Universe (Mezcua et al. 2023). The SMBH mass and accretion rate scales the energetics and mass OF rates of these UFOs (King & Pounds 2003; Tombesi et al. 2013; Matzeu et al. 2023).

Arp 151 (Mrk 40) is a nearby ($z = 0.021$) dwarf galaxy (with a stellar mass of $10^{9.3}\,M_\odot$; Mezcua & Domínguez Sánchez

★ Corresponding author: santanuicsp@gmail.com

2020). It hosts an active SMBH along with two companion galaxies at the same redshift, which indicates that the AGN was likely triggered by the merger event. Optical spectroscopic analyses estimated the BH masses in Arp 151 to be $\sim$4–7 $\times$ $10^6\,M_\odot$ (Bentz et al. 2008; Valenti et al. 2015 and references therein).

The crucial role of nuclear OFs in the feeding and feedback process and in regulating the galaxy growth motivated us to investigate the multi-scale OFs in Arp 151. With the goal of understanding feeding and feedback in dwarf galaxies, we carried out the first detailed X-ray and integral field unit spectroscopic analysis of OFs in the dwarf galaxy Arp 151 using available archival *NuSTAR* and MaNGA data, respectively (see also Vasudevan et al. 2013). The paper is organized as follows: In Sect. 2 we present the X-ray and optical analyses and the UFO and galaxy-scale OF properties. In Sect. 3 we discuss our results and the impact of UFOs in the galaxy feedback, and present our conclusions.

2. Sub-parsec- to galaxy-scale outflows

2.1. Ultra-fast outflow

The X-ray spectroscopic analysis was performed using only *NuSTAR* observations from October 8, 2019, with an exposure time of 24 ks (observation ID 60160430002). No data from other X-ray missions were available. We used standard `nupipeline` and `nuproducts` tasks to extract the spectrum. A source region of 40″ and a background region of 80″ were used in DS9 to extract the spectrum. The source FPMA and FPMB spectra were grouped with a minimum of 15 counts in each bin using the `grppha` task. The spectral modeling for the energy band 3–60 keV was performed in `XSPEC` (v12.12.1; Arnaud 1996) using both phenomenological and physical models. A galactic absorption of $N_H = 1.1 \times 10^{20}$ cm^{-2} (Vasudevan et al. 2013) was used throughout the analysis.

We first fit the data using a simple power-law (`PL`) model along with the line energy shift model `ZASHIFT` and the Gaussian absorption model `GABS` for the absorption line. The best fit with C-stat 67 was achieved for the `PL` photon index, $\Gamma = 1.46 \pm 0.06$. The inclusion of `GABS` improved the fit by reducing ΔC-stat by 9 for a loss of three degrees of freedom, which is equivalent to a $\sim 2\sigma$ detection using F-test probability. This significance does not account for the look-elsewhere effect (Protassov et al. 2002; Gross & Vitells 2010). Interestingly, we observed a tentative blueshifted absorption line at energy $E_{\rm gabs}$ = 8.08 ± 0.24 keV (observer frame) with line width $\sigma_{\rm gabs} = 0.41 \pm 0.27$ keV and line strength 0.45 ± 0.22. The rest-frame energy of the line is 8.25 ± 0.24 keV for $z = 0.021$ in the `ZASHIFT` model. Such absorption lines may originate from the high-velocity outflowing winds, also known as UFOs, often detected in massive AGNs (see Papadakis et al. 2007; Tombesi et al. 2010 for detailed discussions). The left panel of Fig. 1 shows the best-fit model spectra. This phenomenological modeling can give us preliminary information about the spectral shape and absorption line properties. Such a line feature can be identified with highly ionized iron absorption lines associated with Fe XXV or Fe XXVI K-shell transitions. The most plausible assumption is that the observed 8.25 keV line is the blueshifted line corresponding to Fe XXV or Fe XXVI Kα at a rest energy of 6.97 keV. If there is an outflowing wind aligned with our line of sight, a line can be blueshifted. Under that assumption, we calculated the wind velocity using the special relativistic Doppler shift formula $v_w = c[(E/E_{\rm gabs})^2 - 1]/[(E/E_{\rm gabs})^2 + 1]$, which yields $v_w \sim 0.17c$ for $E = 6.97$ keV and $E_{\rm gabs} = 8.25$ keV. We performed the same analysis using FPMB data; however, we could not detect a clear line feature.

To further understand the properties of the outflowing material, we refit the data using the more realistic photoionization model XSTAR (Kallman & Bautista 2001), which can model the absorption line and its properties. For our fitting purposes, we froze the turbulence velocity ($v_{\rm turb}$) to a typical 2000 km s^{-1} (Xrism Collaboration 2025) and generated the table model for $\Gamma = 1.5$. The best fit is achieved with C-stat 68, which is comparable to the phenomenological `GABS` model. The best-fit parameters are $N_H = 2.61^{+6.76}_{-1.23} \times 10^{23}$ cm^{-2}, ionization parameter $\log\xi = 4.5^{+2.0}_{-0.4}$ (the upper hard limit is set to 6.5), and the redshift of the OF ($z_{\rm abs}$) $-0.17^{+0.02}_{-0.01}$. The middle panel of Fig. 1 shows the best-fit spectrum, and the right panel shows the confidence contour between the $\log\xi$ and $z_{\rm abs}$ parameters. The contour indicates that the upper limit of $\log\xi$ is not currently constrained, which may require a longer exposure or higher-S/N data. The best-fit $z_{\rm abs}$ yields an OF velocity of 0.18c, which is remarkably consistent with the estimation from the Doppler shift. The high N_H and ξ indicate that the Fe XXVI Kα likely originated from a high-velocity UFO from the inner region of the disk. The distance of the OF gas can be computed from the best-fit parameters as follows: The minimum distance of the outflowing gas is the radius at which the OF velocity is equivalent to the escape velocity, $r_{\rm min} = 2GM_{\rm BH}/v^2_{\rm UFO} = 6.4 \times 10^{13}$ cm $= 30\ r_S$, for a BH mass of $7.0 \times 10^6\,M_\odot$. Given the above model parameters, the lower limit of the mass OF rate can be estimated as $\dot{M}_{\rm UFO} = \Omega N_H m_p v_{\rm UFO} r_{\rm min} \sim 0.015\,M_\odot$ yr^{-1}, assuming a solid angle $\Omega = 2\pi$ (see Nardini et al. 2015). We further estimated the kinetic power, $\dot{E}_{\rm kUFO} = 1/2\dot{M}_{\rm UFO}v^2_{\rm UFO} \sim 1.4 \times 10^{43}$ erg s^{-1}, and momentum flux rate, $\dot{P}_{\rm UFO} = 5.1 \times 10^{33}$ gm cm s^{-2}.

2.2. Galaxy-scale outflow

We investigated the galactic-scale gas OFs by analyzing the optical integral field spectroscopy data cube from the MaNGA[1] survey.

2.2.1. Outflow velocity

The extent and kinematics of ionized gas OFs are traced using the [O III] λ5007 emission line, which is an excellent tracer of diffuse ionized gas. For this, we first masked the prominent emission features and modeled the stellar continuum in each spaxel by using the publicly available nonlinear optimization spectral fitting routine `PyQSOFit` (Guo et al. 2018). We then fit the [O III] λ5007 emission line using a narrow Gaussian component with a typical width of $\sigma \lesssim 500$ km s^{-1} (Pucha et al. 2025), which represents the emission from the narrow line region. In addition, a broader component for a possible OF signature was introduced for the spaxels where the F-test yields a significantly better fit compared to the single-Gaussian model, with a confidence level of 95%. We further verified this by ensuring a lower Bayesian information criterion value (Schwarz 1978; Liddle 2007) for the double Gaussian profile as compared to the single Gaussian model. Using the OF component, we estimated the typical OF velocity width (W_{80}), which comprises 80% of the flux of the OF component. In addition, the velocity was estimated as $v_{\rm OF} = -v_0 + \frac{W_{80}}{2}$, where v_0 is the velocity offset between

[1] https://magrathea.sdss.org/marvin/galaxy/9000-1901/

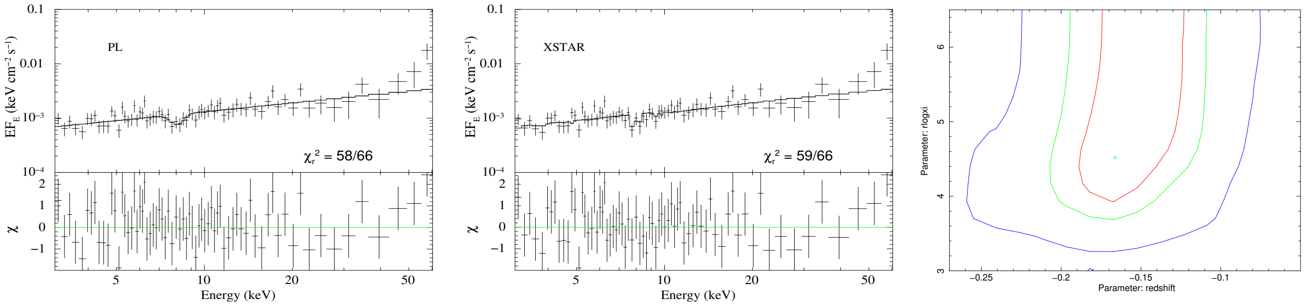

Fig. 1. Best-fit FPMA spectrum of Arp 151 using the `PL` model (*left*) and the XSTAR model (*right*). The solid lines are for the model, and the points with error bars represent the data. The lower subpanels show the residuals of the fit. *Right*: Confidence contour between the wind redshift and ionization parameters. The red, green, and blue lines show the confidence contours at the 1, 2, and 3σ levels.

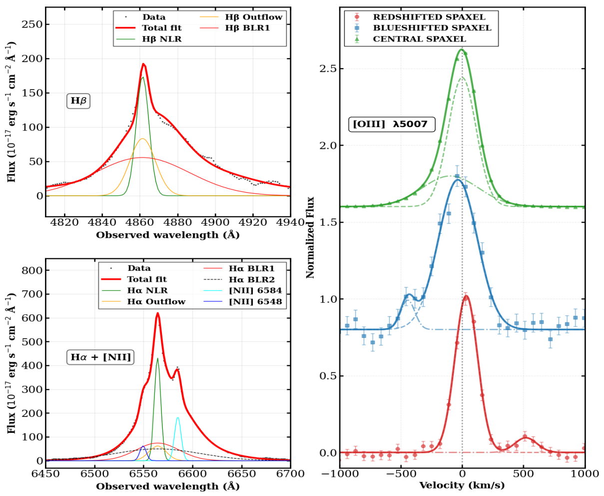

Fig. 2. Multiple Gaussian component spectral line modeling of Hβ (*top left*) and Hα (*bottom left*) emission line profiles. *Right*: [O III] λ5007 nebular emission line modeled with two Gaussian components, for the central spaxel with a weak flow signature and additional two spaxels showing strong blue- and redshifted emission line profiles. The solid line represents the model fit, and the dotted lines represent the individual underlying components.

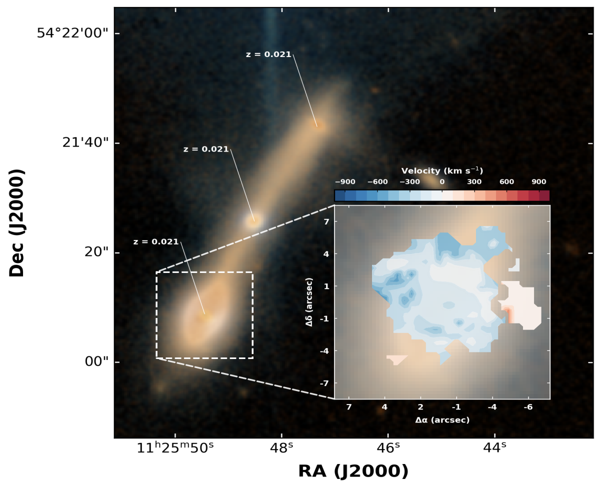

Fig. 3. DECaLS color composite (g-, r-, and z-band) image of the dwarf AGN host galaxy Arp 151. The two companion galaxies both having the same redshift as Arp 151, z = 0.021, indicates the presence of a merger system. The inset shows a bi-conical OF from the dwarf galaxy.

the centers of the narrow and OF components. The [N II] and [S II] doublets were modeled with narrow Gaussian components whose kinematics were tied to the narrow component of the [O III] line. The complex profile of the Hβ and Hα line was fitted with multiple (1–4) Gaussians with an initial guess of two narrow, one broad, and one very broad component. For a physically consistent fit, the width of the narrow components was tied to the [O III] systemic and OF features. To reduce the arbitrariness of the component fits and make the decomposition more physical, we constrained the redshift and width of the two narrow components to be the same as those of the [O III] λ5007 lines. The best-fit model and components for Hβ and Hα emission lines are shown in the left panel of Fig. 2. The full width at half maximum of the Hβ broad emission line component is 3631 ± 717 km s^{-1} as measured from the central region (25 spaxels), where the AGN emission dominates. This yields a M_{BH} of $6.0 \pm 0.2 \times 10^6$ M$_\odot$ (see Greene & Ho 2005 for the scaling relation), which is consistent with other works (Bentz et al. 2008; Valenti et al. 2015) that followed a similar method. The inset in Fig. 3 shows the velocity map, with an apparent biconical outflowing component seen as blueshifted and redshifted profiles (see also Fig. 2, right panel).

2.2.2. Mass outflow rate

The outflowing ionized gas mass (M_{OF}) was estimated using the following relation (Carniani et al. 2024),

$$M_{OF} = 0.8 \times 10^8 \left(\frac{L_{[O\,III],OF}}{10^{44}\,\mathrm{erg\,s^{-1}}} \right) \left(\frac{500\,\mathrm{cm^{-3}}}{n_e} \right) \left(\frac{Z_\odot}{Z} \right) M_\odot, \quad (1)$$

where $L_{[O\,III],OF}$ is the luminosity of the outflowing component of the [O III] λ5007 line, n_e is the electron density, and Z is the gas-phase metallicity. The electron number density was calculated as $n_e = (Cr - AB)/(A - r)$ (Sanders et al. 2016). Here r is the flux ratio of the [S II] emission lines, defined as r = [S II] λ6716/[S II] λ6731, and A, B, and C are dimensionless constants equal to 0.4314, 2107, and 627.1, respectively. The gas-phase metallicity was calculated as $Z/Z_\odot = 4.01^{\mathrm{N2}-0.07}$, where N2 = log ([N II] λ6584/Hα) (see also Carvalho et al. 2020). The estimated mean electron density, r, and metallicity values are 356 cm^{-3}, 1.2162, and 0.64 Z$_\odot$, respectively.

Using the MaNGA 2D OF map, we obtained the mass OF rate as $\dot{M}_{OF} = v_{OF}\, M_{OF}/R_d$, where R_d is the distance of each OF-hosting spaxel from the galaxy center. We detect the extended OF imprints with a physical size of ~2 kpc (4 arcsec) from the galactic center. The average integrated $\dot{M}_{OF}$ and maximum v_{OF} are found to be 0.43 M$_\odot$ yr^{-1} and $\approx \pm 1000$ km s^{-1}, respectively. The magnitudes of massive galaxies with $\dot{M}_{OF}$

of a few $\times$ $10\,M_\odot\,\mathrm{yr}^{-1}$ and v_{OF} of a few $\times$ $10^3\,\mathrm{cm\,s}^{-1}$ are significantly higher, which suggests that OFs in dwarf galaxies are possibly the scaled-down version of those in massive galaxies (Osterbrock & Ferland 2006; Avery et al. 2021; Rodríguez Morales et al. 2025). We estimated the kinetic energy of the galaxy-scale mass OF as $\dot{E}_{\mathrm{kOF}} = 1/2\dot{M}_{\mathrm{OF}}v_{\mathrm{OF}}^2 = 1.4 \times 10^{41}\,\mathrm{erg\,s}^{-1}$ and the momentum flux as $\dot{P}_{\mathrm{OF}} = \dot{M}_{\mathrm{OF}}v_{\mathrm{OF}} = 2.7 \times 10^{33}\,\mathrm{g\,cm\,s}^{-2}$.

To quantify the impact of the UFO and galaxy-scale OF on the host galaxy, we estimated the AGN bolometric luminosity (L_{bol}) using the relation $L_{\mathrm{bol}} = 1000 \times L_{[\mathrm{O\,III}]}$ (Moran et al. 2014). The $L_{[\mathrm{O\,III}]}$ measured over the central 25 spaxels, which is the primary AGN emission at the core and corresponds to a typical seeing of ~2.5 arcsec, results in $L_{[\mathrm{O\,III}]} = 4.1 \times 10^{40}\,\mathrm{erg\,s}^{-1}$ and $L_{\mathrm{bol}} = 4.1 \times 10^{43}\,\mathrm{erg\,s}^{-1}$. The radiation momentum flux is found to be $\dot{P}_{\mathrm{rad}} = L_{\mathrm{Edd}}/c = 2.4 \times 10^{34}\,\mathrm{g\,cm\,s}^{-2}$ for an Eddington luminosity of $L_{\mathrm{Edd}} = 7.2 \times 10^{44}\,\mathrm{erg\,s}^{-1}$ for the BH mass of $\sim 6 \times 10^6\,M_\odot$ taken from this work.

3. Discussion and conclusions

The UFOs launched from the sub-parsec region of the central engine propagate through the interstellar medium and leave their imprint on the galaxy-scale gas dynamics. During this process, they deposit both energy and momentum into the surrounding medium and can potentially affect the star formation of the host galaxy (King & Pounds 2003; Di Matteo et al. 2005; Gaspari et al. 2011; Faucher-Giguère & Quataert 2012). In this work we analyzed *NuSTAR* X-ray data and MaNGA optical data of the nearby dwarf galaxy Arp 151 to understand the sub-parsec- to galaxy-scale OFs and their implications for the host galaxy. We have tentatively detected a UFO signature in the X-ray spectrum based on the detection of an absorption line at ~8.08 keV (observer frame) with $\sim 2\sigma$ confidence. If the absorption line corresponds to Fe XXVI Kα, this would suggest the presence of a highly ionized UFO with $N_H \sim 2.6 \times 10^{23}\,\mathrm{cm}^{-2}$ moving away from the central source with a velocity of $\sim 0.18c$. The combined X-ray and optical analyses raise the question of whether such UFOs in dwarf galaxies are able to produce sufficient feedback. An important parameter that quantifies the feedback contribution of OFs in AGNs is the ratio of the kinetic power of the OF to the bolometric luminosity, ϵ_{UFO} (Di Matteo et al. 2005; Gaspari et al. 2011). For Arp 151, we have estimated $\epsilon_{\mathrm{UFO}} = \dot{E}_{\mathrm{kUFO}}/L_{\mathrm{Edd}} \sim 0.02$, i.e., the $\dot{E}_{\mathrm{kUFO}}$ is 2 percent of L_{Edd}. This ϵ_{UFO} suggests significant feedback from the UFO to the host galaxy. The momentum load of the nuclear OF is $\dot{P}_{\mathrm{UFO}}/\dot{P}_{\mathrm{rad}} = 0.2$, less than that of the radiatively driven winds or OFs from the accretion disk (~1 in King & Pounds 2003).

Moreover, we compared the energy budgets of the galaxy-scale OF and the UFO. The corresponding $\epsilon_{\mathrm{OF}} = \dot{E}_{\mathrm{kOF}}/L_{\mathrm{Edd}} \sim 0.002$ and $\dot{P}_{\mathrm{OF}}/\dot{P}_{\mathrm{rad}} = 0.1$ are lower than the requirements (0.5–5%) typically assumed by the most popular feedback models (Di Matteo et al. 2005; Gaspari et al. 2011). Such a scenario may appear if the cold gas or ionized OFs capture only a tiny fraction of the UFO energy and most of the UFO energy stays in a hot shocked phase while interacting with the ambient medium (see Faucher-Giguère & Quataert 2012; Fiore et al. 2017 for reviews). This can be further verified from the estimation of $\dot{E}_{\mathrm{kOF}}/E_{\mathrm{kUFO}}$ and $\dot{P}_{\mathrm{OF}}/\dot{P}_{\mathrm{UFO}}$. These ratios come out to be ≈0.01 and ≈0.6, which indicates that neither the energy nor the momentum of the UFO has totally transferred to the galactic-scale warm gas; therefore, the galactic-scale OF may be in a momentum-conserving phase.

Our estimated feedback parameter $\epsilon_{\mathrm{UFO}} \sim 0.02$ suggests the UFOs have a significant impact on the host galaxy's feedback mechanism. Such activities have been observed in massive galaxies when they host an AGN. However, no such effects have been reported in the case of dwarf galaxies to date. To further understand the impact of the UFO on the galaxy-scale OFs, we estimated their ratios of energy and momentum rates and found that both the UFO and the galaxy-scale OFs might be in the momentum-conserving phase.

Acknowledgements. MM acknowledges support from the Spanish Ministry of Science and Innovation through the project PID2024-159201NB-C22 and also partly supported by the Spanish program Unidad de Excelencia María de Maeztu CEX2020-001058-M, financed by MCIN/AEI/10.13039/501100011033, and by the MaX-CSIC Excellence Award MaX4-SOMMA-ICE. VRM acknowledges support from the Spanish Ministry of Science, Innovation and Universities through the project PRE2022-104649. This research has utilized the *NuSTAR* Data Analysis Software (NUSTARDAS), jointly developed by the ASI Science Data Center (ASDC), Italy, and the California Institute of Technology (Caltech), USA.

References

Arnaud, K. A. 1996, ASP Conf. Ser., 101, 17
Avery, C. R., Wuyts, S., Förster Schreiber, N. M., et al. 2021, MNRAS, 503, 5134
Barai, P., & de Gouveia Dal Pino, E. M. 2019, MNRAS, 487, 5549
Bentz, M. C., Walsh, J. L., Barth, A. J., et al. 2008, ApJ, 689, L21
Braito, V., Reeves, J. N., Dewangan, G. C., et al. 2007, ApJ, 670, 978
Cappi, M. 2006, Astron. Nachr., 327, 1012
Carniani, S., Venturi, G., Parlanti, E., et al. 2024, A&A, 685, A99
Carvalho, S. P., Dors, O. L., Cardaci, M. V., et al. 2020, MNRAS, 492, 5675
Di Matteo, T., Springel, V., & Hernquist, L. 2005, Nature, 433, 604
Fabian, A. C. 2012, ARA&A, 50, 455
Faucher-Giguère, C.-A., & Quataert, E. 2012, MNRAS, 425, 605
Fiore, F., Feruglio, C., Shankar, F., et al. 2017, A&A, 601, A143
Gaspari, M., Melioli, C., Brighenti, F., & D'Ercole, A. 2011, MNRAS, 411, 349
Greene, J. E., & Ho, L. C. 2005, ApJ, 630, 122
Gross, E., & Vitells, O. 2010, Eur. Phys. J. C, 70, 525
Guo, H., Shen, Y., & Wang, S. 2018, Astrophysics Source Code Library [record ascl:1809.008]
Kallman, T., & Bautista, M. 2001, ApJS, 133, 221
King, A. R., & Pounds, K. A. 2003, MNRAS, 345, 657
Koudmani, S., Henden, N. A., & Sijacki, D. 2021, MNRAS, 503, 3568
Liddle, A. R. 2007, MNRAS, 377, L74
Manzano-King, C. M., Canalizo, G., & Sales, L. V. 2019, ApJ, 884, 54
Matzeu, G. A., Brusa, M., Lanzuisi, G., et al. 2023, A&A, 670, A182
Mezcua, M., & Domínguez Sánchez, H. 2020, ApJ, 898, L30
Mezcua, M., Siudek, M., Suh, H., et al. 2023, ApJ, 943, L5
Mezcua, M., Pacucci, F., Suh, H., Siudek, M., & Natarajan, P. 2024, ApJ, 966, L30
Moran, E. C., Shahinyan, K., Sugarman, H. R., Vélez, D. O., & Eracleous, M. 2014, AJ, 148, 136
Nardini, E., Reeves, J. N., Gofford, J., et al. 2015, Science, 347, 860
Osterbrock, D. E., & Ferland, G. J. 2006, Astrophysics of Gaseous Nebulae and Active Galactic Nuclei (Sausalito, CA: University Science Books)
Papadakis, I. E., Brinkmann, W., Page, M. J., McHardy, I., & Uttley, P. 2007, A&A, 461, 931
Pounds, K. A., Reeves, J. N., King, A. R., et al. 2003, MNRAS, 345, 705
Protassov, R., van Dyk, D. A., Connors, A., Kashyap, V. L., & Siemiginowska, A. 2002, ApJ, 571, 545
Pucha, R., Juneau, S., Dey, A., et al. 2025, ApJ, 990, 231
Rodríguez Morales, V., Mezcua, M., Domínguez Sánchez, H., et al. 2025, A&A, 697, A235
Salehirad, S., Reines, A. E., & Molina, M. 2025, ApJ, 979, 26
Sanders, R. L., Shapley, A. E., Kriek, M., et al. 2016, ApJ, 816, 23
Schwarz, G. 1978, Ann. Stat., 6, 461
Silk, J., & Rees, M. J. 1998, A&A, 331, L1
Sim, S. A., Proga, D., Miller, L., Long, K. S., & Turner, T. J. 2010, MNRAS, 408, 1396
Tombesi, F., Cappi, M., Reeves, J. N., et al. 2010, A&A, 521, A57
Tombesi, F., Cappi, M., Reeves, J. N., et al. 2013, MNRAS, 430, 1102
Valenti, S., Sand, D. J., Barth, A. J., et al. 2015, ApJ, 813, L36
Vasudevan, R. V., Brandt, W. N., Mushotzky, R. F., et al. 2013, ApJ, 763, 111
Xrism Collaboration (Audard, M., et al.) 2025, Nature, 641, 1132